Metallophysics and Advanced Technologies
Металофіз. новітні технол.
Metallofiz. Noveishie Tekhnol.
2023, vol. 45, No. 9, pp. 1083–1097
https://doi.org/10.15407/mfint.45.09.1083
Reprints available directly from the publisher

PACS numbers: 68.49.Jk, 68.49.Sf, 71.45.Gm, 73.20.Mf, 79.20.Uv, 79.40.+z, 82.80.Pv

Effect of Deformation on the Electronic Properties of the W(110) Single Crystals Surface Before and After Different Types of Surface Treatment

S. V. Smolnik[*], I. M. Makeieva[*], V. M. Kolesnyk[*], M. O. Vasylyev[*], M. Ya. Shevchenko[*], I. Ye. Galstian[*,**], E. G. Len[*,***]

[*]*G. V. Kurdyumov Institute for Metal Physics, N.A.S. of Ukraine, 36 Academician Vernadsky Blvd., UA-03142 Kyiv, Ukraine*
[**]*Institute for Solid State Research, Leibniz IFW Dresden, 20, Helmholtz Str., 01069 Dresden, Germany*
[***]*Kyiv Academic University, N.A.S. and M.E.S. of Ukraine, 36 Academician Vernadsky Blvd., UA-03142 Kyiv, Ukraine*

The electronic states' changes on the surface of the W(110) single crystal strained due to plastic bending are studied by the method of plasmon spectroscopy after thermal, thermochemical and ion treatments in comparison with those of analogous unstrained tungsten single crystal. The relative changes of the interplanar spaces, the concentration of the conduction electrons involved in plasma oscillations, as well as work function for electrons are calculated based on the plasmons' energy shifts. As established, the macroscopic bending of the W(110) single crystal leads to a decrease in the work function from its convex surface, which undergoes tensile deformation. The maximal difference in the work functions for unstrained and strained single crystals is observed after all sequentially used thermal, thermochemical and ion treatments and is of 0.2 eV. The obtained results are important for the practical application of thermionic energy converters with nonplanar electrodes.

Corresponding author: Sviatoslav Viktorovych Smolnik
E-mail: sviatsmol@gmail.com

Citation: S. V. Smolnik, I. M. Makeieva, V. M. Kolesnyk, M. O. Vasylyev, M. Ya. Shevchenko, I. Ye. Galstian, and E. G. Len, Effect of Deformation on the Electronic Properties of the W(110) Single Crystals Surface Before and After Different Types of Surface Treatment, *Metallofiz. Noveishie Tekhnol.*, **45**, No. 9: 1083–1097 (2023). DOI: 10.15407/mfint.45.09.1083

Key words: surface of tungsten single crystal, plastic deformation, plasmon spectroscopy, work function, thermionic energy converter.

Методою плазмонної спектроскопії досліджено зміни електронних станів поверхні деформованого за рахунок пластичного вигину монокристалу W(110) після термічного, термохемічного та йонного оброблень у порівнянні з аналогічним недеформованим монокристалом вольфраму. За зсувами енергії плазмонів розраховано відносну зміну міжплощинних віддалей, концентрацію електронів провідности, що беруть участь у плазмових коливаннях, а також роботу виходу електронів. Встановлено, що макроскопічний вигин монокристалу W(110) приводить до зменшення роботи виходу з його опуклої поверхні, яка зазнає деформації розтягнення. Максимальна ріжниця в роботах виходу недеформованого та деформованого монокристалів спостерігається після всіх послідовно реалізованих термічного, термохемічного та йонного оброблень і складає 0,2 еВ. Одержані результати є важливими для практичного застосування термоемісійних перетворювачів енергії з непласкими електродами.

Ключові слова: поверхня монокристалу вольфраму, пластична деформація, плазмонна спектроскопія, робота виходу електронів, термоемісійний перетворювач енергії.

(Received 11 June, 2023; in final version, 20 September, 2023)

1. INTRODUCTION

Currently, the practically single way to convert directly the heat of the high-temperature combustion cycle of nuclear (in the future, thermonuclear) or organic fuel into electricity is the embedding of thermionic converters (TICs) directly into the shells of both the furnaces and the hot zones of reactors [1, 2]. Tungsten single crystals are a promising material for use as cathodes in high-temperature TICs due to their low sublimation rate combined with high emission properties [3]. In order to struggle with the effect of evaporation of the cathode material without deteriorating the technical characteristics of the TIC during all its operation time, it is possible to use two different crystal faces of the same refractory metal single crystal: with larger work function of electron for the cathode manufacturing and with smaller one for the anode manufacturing. In the case of tungsten single crystals, the maximum electron work function is observed for the (110) crystal face [3], which determines the production of TIC cathodes from W(110) single crystals.

It is well known that many important electronic properties of single crystals, including the work function for electrons, are determined by the structure and physicochemical state of their surface layers. Impurities and adsorbates have a significant effect on the value of the work function. Their content on the surface and in the near-surface layers can be controlled by various thermal, thermochemical and radiation

treatments of the samples. Changes in the electronic state of the surface of refractory metals as a result of various types of processing can be studied by the method of plasmon spectroscopy (PS) [4–6]. Based on the determined excitation energies of plasmons (collective vibrations of conduction electrons), it is possible to calculate the concentration of conduction electrons, their work function, as well as the relative change of interplanar spaces depending on external influences on the state of the metal surface.

It is important that, in many cases, especially in compact and mobile nuclear energy sources or power-generating protective shells of future thermonuclear reactors, the TIC electrodes should not be flat, but have a rather complex geometry [7], when the emitter and collector are, for example, coaxial cylinders or tori with a small interelectrode gap. It is known that the adsorption capacity and high-temperature strength of cylindrical electrodes can be significantly increased if, instead of cylinders machined from a single crystal rod, the used cylinders are obtained by plastic deformation of crystallographically oriented plate with subsequent electron beam welding of the joints after it wrapping onto the surface of a given geometry [7]. The increase in high-temperature strength is due to the formation during plastic deformation of a high (up to 10^9 cm^{-2}) redundant density of dislocations of the same sign and its preservation up to pre-melting temperatures during stabilizing annealing [8]. Therefore, it is topical to study the electronic properties (especially the work function) of the working surfaces of TIC electrodes made from real deformed single crystals of refractory metals in comparison with unstrained ones, as well as the effect of various types of physicochemical treatments on them.

In connection with the above, the goal of this work is a comparative study using the method of plasmon spectroscopy of changes in the electronic state of strained by plastic deformation and unstrained single crystals of W(110) fabricated from the same single crystal rod, which subjected to thermal, thermochemical, and ion treatments at the same conditions.

2. RESEARCH OBJECTS AND METHODOLOGY

The plasmon excitation features in the secondary electron emission spectra has been studied for two samples of tungsten single crystal. Both samples were prepared from a single crystal strip of W(110) cutting with an accuracy of $\pm 20'$ from a single crystal rod grown by the electron beam crucibleless zone recrystallization method.

An unstrained sample of W(110) with a diameter of 10 mm and a thickness of 2 mm was cut from a single crystal by the electrospark method and subjected to further mechanical grinding and electropolishing from the side of the investigated surface. The deformed

W(110)-*D* sample has a form of plastically strained single crystal strip of 2 mm thick wrapped around a cylindrical surface with a radius of 14 mm. A detailed description of the preparation of this sample is given in Ref. [9]. The convex side of this sample, which was subjected to tensile stress during bending, was investigated. That is the convex side, which is used for electrons emitting in the case of the placement of nuclear fuel inside cylindrical capsules. Such devices can to supply for a long time with electricity the spaceships, submarines, and other objects, which have a problem with access to sunlight and organic fuels. In the case of a thermonuclear reactor, the inside torus of the protective shell (which can be immediately made double-layered) can use as a TIC cathode with emitting external convex side.

Preliminary, the W(110) and W(110)-*D* samples were subjected to step heating in the temperature range of 900–2400°C in a vacuum not lower than $5 \cdot 10^{-7}$ Pa. The determination of the content of impurities in single crystals of tungsten was carried out by the method of secondary ion mass spectrometry (SIMS) [10] in an ultrahigh vacuum facility using a liquid metal ion source [11]. The working substance for obtaining the initial ion current was liquid gallium. The diameter of Ga^+ ion beam was $\cong$ 10 μm, and the energy and density of the initial current were 9 keV and $1 \cdot 10^{-2}$ A·cm^{-2}, respectively. After heating at a certain temperature, the samples were cooled down during 15–20 minutes. Then, within 30 minutes, the surface of the samples was cleaned by the scanning beam of gallium ions. As a result of cyclic annealing and ion beam cleaning of the unstrained sample and after 30 minutes of heating at a temperature of 2400°C, all impurities were removed from the near-surface region, except carbon, the content of which, according to chemical analysis, did not exceed $1 \cdot 10^{-3}$ mass.% (Fig. 1, *a*). For the deformed sample, after a similar heat treatment, small peaks of carbon and oxygen impurities were observed near the sensitivity limit of the mass analyser, but an abnormally high amount of ionized water molecules was detected, which had been observed up to extremely high temperatures (2400°C) (Fig. 1, *b*).

The presence of adsorbed water in the surface layers and in the volume of heated metal samples is well known, but it is easily desorbed at a temperature of 530°C [9]. The formation and preservation of ionized water up to high temperatures in the volume of plastically deformed tungsten single crystal is probably related to the presence of a high density of dislocations of the same sign, stable up to the pre-melting temperature [8]. The probable cause of water entering into the volume of the single crystal is an insufficiently high vacuum ($7 \cdot 10^{-3}$ Pa) in the electron beam-welding chamber. When a single crystal plate is heated by an electron beam, water molecules can easily ionize and in this state enter into dislocation cores of the tungsten lattice, which are potential wells for these impurities [9]. The presence of O^+ and WO^+ peaks in the

secondary ion mass spectrum indicates an increased content of oxygen in dislocations at the surface of the deformed single crystal, which persists at least up to temperature of 2400°C.

The presence of ionized molecules of water in the surface layer of a deformed tungsten sample after high temperature annealing and ion etching is unusual, since it is known from studies of flat samples that all impurities, except carbon, are removed at high temperatures [12]. Subsequently, it is the heat-stimulated segregation of impurity carbon atoms from the volume to the surface of a flat tungsten single crystal that determines the sublimation and electronic properties of its surface. It is also worth noting the following. The C atoms are practically absent in the surface of deformed tungsten (Fig. 1, *b*). This may be due to the blocking of C atoms by ionized water molecules in a dislocation core. The formation of additional dislocations during the plastic deformation of a tungsten single crystal with the trapping of ionized molecules of water by them, can probably become a new effective method of obtaining surfaces of tungsten single crystals that would not contain carbon impurities.

All measurements by the method of plasmon spectroscopy were performed in ultra-high vacuum using a low-energy electron spectrometer at an operating pressure of residual gases not worse than $1 \cdot 10^{-7}$ Pa. The spectrometer is equipped with a four-grid hemispherical energy analyser, as well as electron and ion guns [13]. For peaks' separation in the spectrum of secondary electrons, the method of one-shot differentiation of the secondary current delay curve was used by recording the signal of the first harmonic of the collector current when the delay potential is modulated by a sinusoidal voltage [14]. The error in measurement of intensity and energy of surface and volume plasmons did

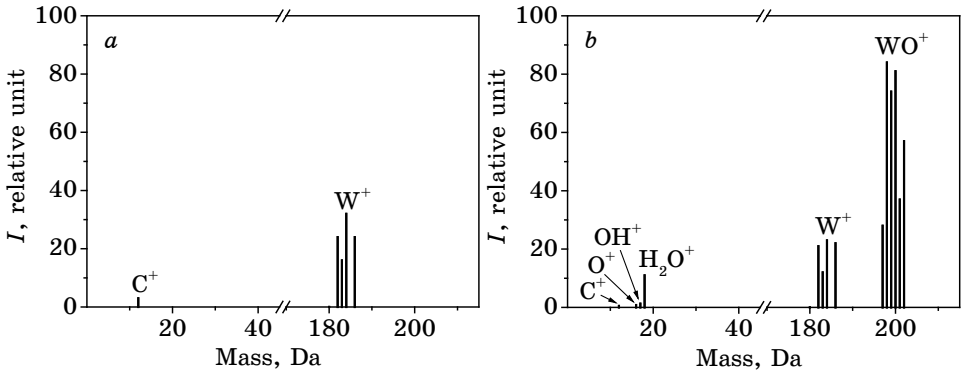

Fig. 1. Mass spectra of secondary ions of W(110) single crystals after cleaning with an ion beam and heating at a temperature of 2400°C for 30 min: *a*—undeformed plate; *b*—the convex side of a plastically deformed plate [9] (masses are measured in daltons (unified atomic mass unit)).

not exceed 5% .

During the experimental studies directly in the chamber of the electron spectrometer, the surfaces of the W(110) and W(110)-*D* samples were sequentially subjected to the following treatments: 1—annealing at a temperature of 1750°C for 540 min; 2—exposure in atomic oxygen at its pressure $P_{O_2} = 8 \cdot 10^{-4}$ Pa at a temperature of 1700°C for 180 min; 3—cleaning of the surface with argon ions with an energy of 800 eV and a current density of 5 μA·cm^{-2}; 4—annealing at a temperature of 1750°C for 200 min.

To obtain atomically pure oxygen, the copper oxide was pressed into a thin-walled platinum tube, and pure oxygen was released during it heating [15].

To study the effect of ion bombardment on the electronic properties of single crystals, an ion gun with ionization of the working gas by electron impact was used. Spectrally pure argon was used as the working gas.

After each type of surface treatment of the samples, the spectra of electrons' energy characteristic losses were recorded, the subsequent analysis of which provided data on the electronic properties of the surface.

3. RESULTS AND DISCUSSION

For experimental determination of the excitation losses because of surface and bulk plasmons, the electrons' energy loss spectra were recorded in the energy range of the primary electrons E_0 from 50 to 650 eV. In this case, the thickness of the investigated layer is 1.0–5.0 nm [16].

The Table 1 shows the averaged experimental energy values of surface $E_s = \hbar\omega_s$ and bulk $E_b = \hbar\omega_b$ plasmons (ω_s and ω_b are the oscillation frequencies of surface and bulk plasmons, respectively) after different types of step-by-step surface treatments of unstrained and deformed W(110) single crystals.

It is known that the bulk plasmon energy can be estimated within the free electron gas model according to the formula [17]

$$E_b = \hbar \sqrt{\frac{e^2 n}{m^* \varepsilon_0}}, \qquad (1)$$

where n is the density of valence electrons, e is the charge of an electron, m^* is the effective mass of electron, and ε_0 is the dielectric constant of vacuum.

If we assume that all valence electrons in the b.c.c. tungsten crystal (electronic configuration [Xe]$5d^4 6s^2$) are free and participate in plasmon oscillations, then, according to Eq. (1), we can obtain an estimation of $E_{b1} \cong 22.85$ eV. In the initial state, the bulk plasmon energy E_b

of the unstrained W(110) single crystal is close to the value of E_{b1} (see Table 1). The treatment of the surface of the W(110) single crystal at different regimes significantly increases the value of E_b compared to E_{b0}. The increase of the E_b values is a consequence of the increase of the electron concentration for b.c.c. tungsten at all processing modes used in the work compared to the initial state.

After annealing at a temperature of 1750°C for 540 min, the value of E_b increases by 0.4 eV (Table 1). Since all impurities, except carbon, are removed from the tungsten single crystal under such annealing conditions [12], the reason for this behaviour of E_b can only be the thermally stimulated segregation of impurity carbon atoms from the volume to the surface of the tungsten single crystal. The increase in electron density and the increase in E_b values should also be caused by the compressive microdeformation caused by defects (compared to the initial sample) in the near-surface layer of the macroscopically unstrained W(110) single crystal (Fig. 1). Tensile deformation has an inverse effect on E_b, which can be observed in the example of a macroscopically deformed W(110)-*D* single crystal (the convex side of the sample was studied).

The holding in atomically pure oxygen at a temperature of 1700°C does not significantly change the value of the bulk plasmon energy compared to the data obtained after the previous annealing stage. On the other hand, the bombardment of the surface with low energy Ar^+ ions leads to a certain decrease of the E_b values compared to the previous state, probably due to the formation of vacancy-type radiation defects and the removal of carbon from the near-surface layer and the processes of crystal lattice relaxation in it [18]. After the final annealing at a temperature of 1750°C for 200 minutes, the maximal effect of increasing the bulk plasmon energy of the unstrained W(110) single

TABLE 1. The average values of the surface (E_s) and bulk (E_b) plasmon energy (eV) for strained and unstrained W(110) single crystals.

Plasmon energy	Sample	Surface treatment modes				
		0	1	2	3	4
		Initial state	Annealing at 1750°C for 540 min	Exposure in O_2 at 1700°C for 180 min	Ion etching (Ar^+)	Annealing at 1750°C for 200 min
E_s, eV	W(110)	9.18	8.12	8.65	7.90	7.10
	W(110)-*D*	12.70	13.10	11.50	11.60	12.20
E_b, eV	W(110)	22.80	23.20	23.25	23.11	23.90
	W(110)-*D*	23.10	22.20	22.50	22.40	22.10

crystal is observed.

For the W(110)-*D* sample deformed by plastic bending in the initial state, a shift of the bulk plasmon energy by 0.3 eV towards higher energies is observed compared to the unstrained W(110). The presence of a distorted crystal lattice, ionized water in the dislocation core, and the presence of adsorbed particles on the surface lead to an increase in E_b value. After the first heat treatment of the W(110)-*D* surface, the value of E_b decreases significantly and then practically does not change after all successive modes of sample treatment.

The surface plasmon energy for all surface states of a deformed tungsten single crystal exceeds the surface plasmon energy of an unstrained sample. The case of a deformed crystal after the first heat treatment (with $E_b/E_s = 1.69$) is closest to the theoretical estimation of the ratio of bulk and surface plasmon energies ($E_s \approx E_b/\sqrt{2}$) [17]. However, it, as well as other cases, for which $E_b/E_s = 1.81–3.37$, is quite far from the estimated value of $\sqrt{2}$. This indicates the significant influence of effects not considered in the gas model of free electrons, such as impurities, microscopic and macroscopic deformations, and the chosen crystallographic direction, on the real energy values of both types of plasmons and on the relationship between them.

It is worth noting that the use of free electron gas approximation in the analysis of experimental data for metal, obtained within the framework of the method of electron energy characteristic losses, leads to the description of the dielectric permittivity of the medium by the Drude's formula: $\varepsilon(\omega) = 1 + \omega_b^2/\omega^2$. This approximation works well at high frequencies ($\omega >> \tau^{-1}$, τ is the relaxation time of the free electron gas, which at room temperature is of the order of 10^{-14} s), when the attenuation is small ($\mathrm{Im}\varepsilon \cong 0$). For elementary metals, the last condition is fulfilled, but for transition metals, due to the overlap of the *s*–*p* and *d* bands and the corresponding interband transitions, the condition $\mathrm{Im}\varepsilon \cong 0$ does not hold, which leads to the shifting and broadening of plasmon lines for the *s*–*p* electron subsystem, as well as to the 'joining' of the branches of the dispersion curve for bulk and surface plasmons (the energy gap disappears), but with a certain preservation of other characteristic features of separate areas that would correspond to two types of plasmons in the absence of significant attenuation. In the case of sufficiently low frequencies ($\omega << \tau^{-1}$), the approximation of the free electron gas (Drude's model) can be used until the condition $\lambda << \delta = c(2\pi\sigma\omega)^{-1/2}$ is fulfilled [19]. Here, λ is the average length of the electron free path, δ is the thickness of the skin layer, *c* is the speed of light in a vacuum, $\sigma = ne^2\tau/m^* = \omega_b^2\tau/(4\pi)$ is the specific electrical conductivity. At the same time, the energy transferred from primary electrons to metal electrons should correspond to the excitation of bulk plasmon oscillations (with $\mathrm{Im}\varepsilon \cong 0$): $E \cong 20–30$ eV [17]. Note that, for $E \cong 2–3$ eV, the contribution to the spectrum of energy characteristic

losses is mainly made by interband electron transitions. Above, we were talking about transverse plasmons. However, the consideration of longitudinal plasmons does not change the general picture, since according to experimentally determined not very large transmitted pulses they are also excited in the first approximation in the vicinity of the frequency ω_b [19]. The given considerations substantiate the applicability of Drude's formula not only for bulk but also for surface plasmons, the frequency of oscillations of which at not very small wavelengths are in the vicinity of the frequency $\omega_s \approx \omega_b/\sqrt{2}$ [17, 19]. In the same approximation, for sufficiently large values of the longitudinal wave number and for the macroscopic dimensions of the sample, it becomes possible to use the same formulas as for a flat surface in the case of a cylindrical surface of the (deformed) sample [19]. In the experiment for tungsten, the peaks of bulk and surface plasmons are clearly defined. Their relatively small width indicates that in this case the plasmons are well-defined quasiparticles. The deviations of the peaks' energy position from the estimated values (E_{b1} and $E_{b1}/\sqrt{2}$) are related not so much to the dispersion dependence $\omega(\mathbf{k})$ (this issue requires additional research, as well as the issue of deviation from the Drude's model), but to a change in the chemical composition, defect structure in the near-surface layer, and macroscopic deformation of the sample. Moreover, since different methods give significantly different absolute values of the work function, we are mainly interested in the magnitude of changes in the plasmon energy and the corresponding work function due to various types of processing and deformation. Therefore, in the framework of such consideration, all effects associated with deformation, defects, and other deviations from perfection (and isotropy; see work [4] for the W(100) surface) are reduced only to a certain change in interatomic distances and, accordingly, in electron concentration n.

Based on the principles outlined above and in Ref. [17], *i.e.*, assuming that the change in plasmon energy is related only to the change in electron concentration caused by the deformation of the crystal lattice, it is possible to calculate the relative changes in interplanar distances $\Delta d/d$ through the plasmon energy shifts using the formula:

$$\Delta d/d = -2\Delta E/E_b, \tag{2}$$

where $\Delta E = E_b - E_{b0}$ is the plasmon energy shift of the initial sample (E_{b0}) as a result of thermal, chemical and/or ion treatment of the latter, E_b is the averaged bulk plasmon energy after the corresponding impact on the sample.

As can be seen from Fig. 2, for the W(110)-*D* sample, positive values of the relative change in interplanar distances are observed for all processing modes compared to the initial state of the deformed sample.

The maximum increase in interplanar distances for the W(110)-*D* sample is observed after the final annealing at a temperature of 1750°C for 200 minutes (Fig. 2). For the unstrained sample, contrariwise, the effect of crystal lattice compression due to the diffusion of carbon atoms to the single crystal surface is observed after each surface treatment (Fig. 2). In this case, the relative deformations of the near-surface atomic layers of the W(110) sample for each treatment mode are several times larger by modulus than for the W(110)-*D* sample under the same treatment. The maximum reduction in interplanar distances is observed after cleaning the surface of the unstrained W(110) sample with low-energy Ar^+ ions, which is probably associated with perturbations in the atomic structure due to the formation of radiation defects and the implantation of Ar^+ ions in a single crystal.

As the interplanar distance d increases, the concentration of free electrons in the near-surface layer should decrease, and thus, the energy of the plasma oscillations should decrease too that is observed in the experiment for bulk plasmons of the W(110)-*D* sample (Fig. 2, Table 1). In contrast, for the unstrained W(110) sample, the interplanar distance decreases in all processing modes (Fig. 2) and the energy of bulk plasmons increases compared to the initial state of the sample (Table 1). The presence of plastic deformation in the W(110)-*D* sample leads to an additional increase in interplanar distances on its convex surface compared to the unstrained sample, resulting in lower E_b values for the W(110)-*D* single crystal than for W(110). This regularity occurs for all

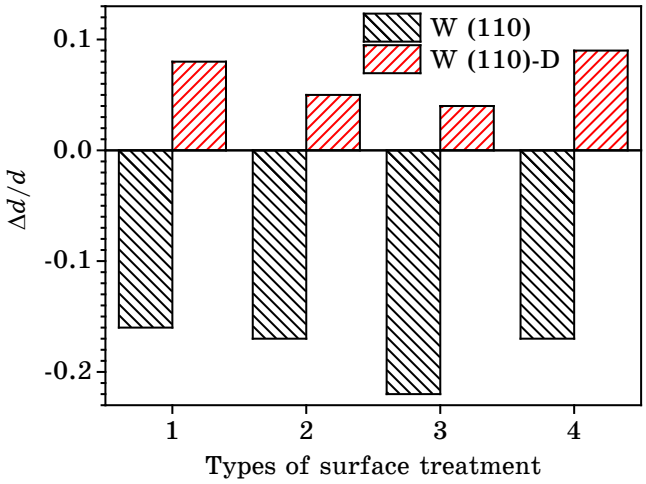

Fig. 2. Changes of interplanar spacing after various modes of the surfaces treatment; 1—annealing at 1750°C for 540 min; 2—exposure in oxygen at 1700°C for 180 minutes; 3—bombardment by Ar^+ ions; 4—annealing at 1750°C for 200 min.

treatment modes of the W(110)-*D* and W(110) samples (see Table 1), but it does not extend to these samples in the initial non-equilibrium state.

From Eq. (1), one can obtain an expression to calculate the concentration of conduction electrons n_p participating in surface and bulk plasma oscillations:

$$n_p = 0.724 \cdot E_p^2 \cdot 10^{21} \text{ cm}^{-3}, \quad (3)$$

where E_p is the surface (p = s) and bulk (p = b) plasmon energy, respectively. The concentrations of conduction electrons n_p (p = s, b) near the surface of the W(110) and W(110)-*D* samples are calculated from both the surface and bulk plasmon energies and shown in the Table. 2.

The concentration of conduction electrons according to the surface plasmon data decreases significantly for both samples, which is associated with the features of surface relaxation and the presence of defects in the surface structure. It should also be noted that n_s for W(110)-*D* is 2–3 times higher than the similar value for W(110), which indicates greater distortions of the surface layers of an unstrained single crystal compared to a plastically deformed one (which is also indicated by the analysis of the value of $\Delta d/d$, Fig. 2).

For the W(110) sample in the initial state, the conduction-electrons' concentration calculated from the bulk plasmon energies coincides with the value calculated by the free electron model and is equal to 6 electrons per atom (this is also an argument in favour of the applicability of the Drude's model). After successive surface treatments, an increase in the conduction electron concentration is observed due to the growth of compressive deformation in the W(110) near-surface layer. A certain increase in n_b in the initial state of the W(110)-*D* sample compared to the conduction electron concentration for the unstrained W(110) is associated (as well as the behaviour of the E_b value discussed above) with the deformation of the crystal lattice and the presence of ionized water and other defects in the volume and on the surface of the samples (see Fig. 1). As a result of the interplanar-distances' increasing after surface treatments of the W(110)-*D* single crystal, the con-

TABLE 2. Values of the conduction electrons' concentrations ($n_{s,b}$), el./atom (the treatment modes one can see in Table 1).

Plasmon type	Sample	Surface treatment modes				
		0	1	2	3	4
Surface	W(110)	0.97	0.77	0.86	0.72	0.57
	W(110)-*D*	1.87	1.95	1.50	1.55	1.70
Bulk	W(110)	6.0	6.24	6.24	6.18	6.60
	W(110)-*D*	6.16	5.70	5.86	5.84	5.65

centration of conduction electrons decreases and the covalent bond weakens [15], which should lead to a decrease in the work function of electrons from the surface. The maximum effect of n_b decrease occurs after the final annealing of the W(110)-*D* single crystal at a temperature of 1750°C for 200 min.

According to Ref. [20], the work function is connected with the bulk plasmon energy by the following relationship:

$$\varphi = 1.8 + (1/9)E_b. \quad (4)$$

The results of the corresponding calculations are shown in Fig. 3. As can be seen from this figure, for the unstrained sample in the initial state, the work function of electron from the (110)W surface is equal to 4.33 eV. After annealing at a temperature of 1750°C for 540 min, the work function increases to 4.38 eV, and after exposure in oxygen and bombardment with Ar^+ ions, it practically does not change. After final annealing at 1750°C, the value of φ rises sharply to a maximum of 4.46 eV. Heat treatment at temperatures of 1700 and 1750°C obviously leads, as mentioned above, to the activation of carbon diffusion and its segregation from the bulk to the surface of the W(110) crystal, which is reflected in a consistent increase in work function after surface treatments.

The surface of the deformed W(110)-*D* single crystal (Fig. 3) in its initial state has a rather large electron work function (4.37 eV), indi-

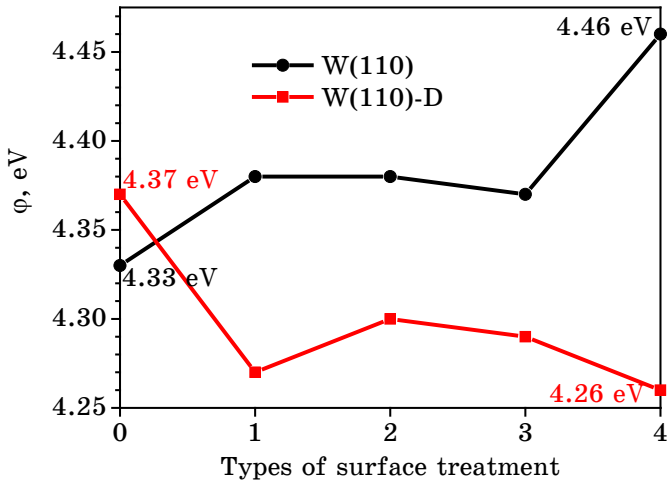

Fig. 3. Electron work function from the strained and unstrained surfaces W(110): 0—in the initial state; 1—after annealing at 1750°C for 540 minutes; 2—exposure in oxygen at 1700°C for 180 minutes; 3—bombardment by Ar^+ ions; 4—annealing at 1750°C for 200 min.

cating its non-equilibrium state and the presence of adsorbed particles on it. Annealing of the W(110)-*D* sample at a temperature of 1750°C for 540 min results in a sharp decrease of the work function to 4.27 eV. Further exposure in atomic oxygen increases the work function to 4.30 eV. Cleaning the surface with Ar^+ ions followed by annealing at a temperature of 1750°C for 200 min again leads to a decrease in the work function to a minimum value of 4.26 eV. It is important to note that after all treatments, the work function on the surface of a deformed single crystal is significantly less than the work function on the unstrained W(110) crystal. As shown above, in all modes of W(110)-*D* surface treatment, the interplanar distances are increased relative to the initial state, which, in turn, leads to a weakening of the covalent bond [15] and a decrease in the work function of electron.

Thus, the plastic deformation of the W(110) single crystal in the initial state slightly increases the electron work function for the emitting (convex) surface from 4.33 to 4.37 eV. Such increase can be caused by the non-equilibrium state of the deformed surface.

For all types of thermal, thermochemical and ionic treatments of a plastically deformed sample, the work function decreases in relation to both the initial deformed state and the unstrained sample after the same surface treatment. This is in accordance with the results of [21] regarding the general laws of the influence of deformation on the work function in metals. The maximum difference in the work function of deformed and unstrained single crystals is observed after the whole complex of successive thermal, thermochemical, and ionic treatments and is of 0.2 eV.

As can be seen from the above, the reason for the lower values of the work function at the surface of the deformed single crystal is the increase in the average value of the crystal lattice period of tungsten due to the appearance of dislocations during plastic deformation and the corresponding decrease in the interatomic interaction force. An important role in the formation of the electronic properties of an unstrained tungsten single crystal is played by the diffusion of C atoms from the volume to the surface, while the properties of a plastically deformed sample are more influenced by ionized water molecules captured by the nuclei of dislocations during the sample preparation stage.

4. CONCLUSIONS

1. Plastic deformation of the W(110) single crystal, which occurs, for example, due to its cylindrical bending during the formation of a closed TIC capsule with nuclear fuel or a thermonuclear reactor shell, slightly increases the work function of electron from the emitting convex surface (from 4.33 to 4.37 eV), despite the presence of macroscopic

tensile deformation. This growth is caused by non-equilibrium states of the deformed and unstrained surfaces of the W(110) single crystal and determines the need for thermal and other sample treatments before its practical use.

2. After all the above successive treatments, the deformed and unstrained samples pass into more equilibrium states that is accompanied by a restructuring of their surface and a change in the corresponding electronic properties. Thus, at high temperatures, carbon diffusion is activated in the unstrained sample and its segregation occurs from the bulk to the surface of the W(110) single crystal, which is reflected in a decrease of the interplanar distance in the near-surface layer leading to a local increase of the electron concentration and the work function after the selected successive surface treatments. Ion etching slightly breaks the monotony of this dependence due to the formation of additional radiation defects. For the plastically deformed sample W(110)-*D*, all successive treatments lead to a significant relaxation of macro- and microstrains. An important role in the formation of the electronic properties is played the presence of a high density of dislocations of the same sign (up to 10^9 cm^{-2}) and ionized water molecules captured by dislocations at the stage of sample preparation. All treatments lead to an increase in the interplanar distances in the near-surface layer, a local decrease in the electron concentration, and a corresponding decrease in the work function of the convex side of the plastically deformed W(110) single crystal relative to both the initial state of the W(110)-*D* sample and the unstrained sample after the same surface treatments.

3. The maximum difference in the values of work function of unstrained and deformed crystals is observed after the whole complex of sequentially performed thermal, thermochemical and ion treatments and is 0.2 eV, which is important to consider for designing thermionic energy converters with cylindrically deformed electrodes.

4. The practically absence of carbon atoms on the surface of deformed tungsten sample can be caused by the blocking of carbon segregation to the surface by ionized water molecules in the dislocation nuclei. The formation of additional dislocations during plastic deformation of a sample, together with ionized water molecules capturing by them, can become a new effective method of obtaining surfaces of single crystals of refractory metals and their alloys, which would not contain carbon impurity.

ACKNOWLEDGMENTS

This work was supported by projects Nos. 0119U001167 and 0123U102275 of the National Academy of Sciences of Ukraine, and partially by UKRAPRO scholarship program for Ukrainian researchers (Volkswagen Foundation).

REFERENCES

1. M. F. Campbell, T. J. Celenza, F. Schmitt, J. W. Schwede, and I. Bargatin, *Adv. Sci.*, **8**: 2003812 (2021).
2. A. V. Belkin and N. V. Schukin, *Phys. Atom. Nuclei*, **84**: 1522 (2021).
3. V. S. Fomenko, *Ehmissionnyye Svoistva Materialov: Spravochnik* [Emission Properties of Materials: Handbook] (Kiev: Naukova Dumka: 1981) (in Russian).
4. M. O. Vasylyev, E. G. Len, V. M. Kolesnik, I. M. Makeeva, V. I. Patoka, and S. V. Smolnik, *Metallofiz. Noveishie Tekhnol.*, **42**, No. 4: 471 (2020) (in Russian).
5. M. A. Vasylyev and V. A. Tinkov, *Surface Review and Letters*, **15**, No. 5: 635 (2008).
6. M. O. Vasylyev, V. M. Kolesnik, S. I. Sidorenko, S. M. Voloshko, V. V. Yanchuk, and A. K. Orlov, *Metallofiz. Noveishie Tekhnol.*, **40**, No. 7: 919 (2018) (in Ukrainian).
7. L. V. Demchenko, A. I. Dekhtyar, and V. A. Kononenko, *Металлофизика*, **6**, № 3: 112 (1984) (in Russian).
8. L. V. Demchenko, A. I. Dekhtyar, and A. P. Starzhinskij, *Phys. Met. Metallog.*, **80**, No. 3: 312 (1995).
9. A. I. Dekhtyar, V. N. Kolesnik, V. I. Patoka, and N. A. Shevchenko, *Metallofiz. Noveishie Tekhnol.*, **23**, No. 3: 335 (2001) (in Russian).
10. V. T. Cherepin and M. A. Vasil'ev, *Metody i Pribory dlya Analiza Poverkhnosti Materialov: Spravochnik* [Methods and Instruments for Surface Analysis of Materials: Handbook] (Kiev: Naukova Dumka: 1982) (in Russian).
11. G. G. Managadze, V. T. Cherepin, Y. G. Shkuratov, V. N. Kolesnik, and A. E. Chumikov, *Icarus*, **215**, No. 1: 449 (2011).
12. V. I. Patoka, *Doslidzhennya Parametriv Vyparovuvannya Tugoplavkykh Metaliv ta Yikh Splaviv u Nadvysokomu Vakuumi* [Study of Evaporation Parameters of Refractory Metals and Their Alloys in Ultrahigh Vacuum] (Disser. for Cand. Phys.-Math. Sci.) (Kyiv: G. V. Kurdyumov Institute for Metal Physics, N.A.S.U.: 2020) (in Ukrainian).
13. M. A. Vasil'ev and S. D. Gorodetsky, *Vacuum*, **37**: 723 (1987).
14. V. A. Tinkov, M. A. Vasylyev, and G. G. Galstyan, *Vacuum*, **85**: 677 (2011).
15. I. Ya. Dekhtyar, V. N. Kolesnik, V. I. Patoka, and V. I. Silantiev, *DAN USSR, Ser. A*, No. 12: 1124 (1975) (in Russian).
16. V. E. Korsukov, A. S. Luk'yanenok, and V. N. Svetlov, *Poverkhnost'. Fizika, Khimiya, Mekhanika*, No. 11: 28 (1983) (in Russian).
17. D. Pines, *Elementary Excitation in Solids* (New York: Benjamin Press: 1963).
18. M. A. Vasylyev, S. P. Chenakin, and V. A. Tinkov, *Vacuum*, **78**: 19 (2005).
19. V. V. Klimov, *Nanoplasmonics* (Moskva: Fizmatlit: 2010) (in Russian).
20. E. A. Bakulin and M. M. Bredov, *Fiz. Tverd. Tela*, **12**, No. 3: 891 (1977) (in Russian).
21. W. Li and D. Y. Li, *Phil. Mag.*, **84**, No. 35: 3717 (2004).